Electrostatic Solitary Waves in Relativistic Degenerate Electron–Positron–Ion Plasma

Ata ur Rahman, Ioannis Kourakis, and Anisa Qamar

***Abstract*— The linear and nonlinear properties of ion acoustic excitations propagating in warm dense electron–positron–ion plasma are investigated. Electrons and positrons are assumed relativistic and degenerate, following the Fermi–Dirac statistics, whereas the warm ions are described by a set of classical fluid equations. A linear dispersion relation is derived in the linear approximation. Adopting a reductive perturbation method, the Korteweg–de Vries equation is derived, which admits a localized wave solution in the form of a small-amplitude weakly super-acoustic pulse-shaped soliton. The analysis is extended to account for arbitrary amplitude solitary waves, by deriving a pseudoenergy-balance like equation, involving a Sagdeev-type pseudopotential. It is shown that the two approaches agree exactly in the small-amplitude weakly super-acoustic limit. The range of allowed values of the pulse soliton speed (Mach number), wherein solitary waves may exist, is determined. The effects of the key plasma configuration parameters, namely, the electron relativistic degeneracy parameter, the ion (thermal)-to-the electron (Fermi) temperature ratio, and the positron-to-electron density ratio, on the soliton characteristics and existence domain, are studied in detail. Our results aim at elucidating the characteristics of ion acoustic excitations in relativistic degenerate plasmas, e.g., in dense astrophysical objects, where degenerate electrons and positrons may occur.**

***Index Terms*— Plasma oscillations, plasma waves.**

I. Introduction

RECENTLY there has been a great deal of interest in elucidating the dynamics of collective processes in degenerate dense plasmas, commonly found in dense astrophysical objects (e.g., white and brown dwarfs, neutron stars, and magnetars), in the core of giant planets (e.g., Jovian planets), which can also be produced in the next generation of laser-based matter compression schemes [1]–[5]. In degenerate plasmas, physical parameters like density, magnetic field, and temperature vary over a wide range of values. For example, the degenerate electron number density may exceed the solid matter density by many orders of magnitude in white dwarfs, neutron stars, and in the next generation of inertially compressed materials in intense laser-solid target interaction experiments [4]. The magnetic field is estimated to vary from a few kilogauss to a few gigagauss (or even petagauss) in white dwarfs (neutron stars, respectively), and temperatures can be as high as in fusion plasma ($\sim 10^8$ K) [5]. Under such conditions, quantum degeneracy and relativity effects are ubiquitous because the thermal de Broglie wavelength is of the order of or greater than the inter-fermion distance. Quantum effects of lighter species (electrons, positrons, and so on) are more prominent due to their smaller mass than those of heavier (ion) species, which may behave classically or quantum mechanically depending upon the degeneracy parameter $n\lambda_B^3$, which should be larger than unity for quantum effects to be significant, where n denotes the particle number density [5]. At extremely high densities, the electron Fermi energy $E_{\mathrm{Fe}0}$ can be much larger than thermal energy, so that the electron thermal pressure can be disregarded with respect to the Fermi degeneracy pressure. The Fermi degeneracy pressure arises due to the combined effect of Pauli's exclusion principle and Heisenberg's uncertainty principle. The degenerate electrons may be nonrelativistic, relativistic, or ultrarelativistic depending upon the ratio of the Fermi energy to the rest mass energy of electron. For degenerate electrons, Chandrasekhar [6], [7] has employed an equation of state (EoS) to estimate the critical mass limit of white dwarf stars. The role of the relativistic and degenerate electron pressure and its consequences are thus effectively modeled, spanning a wide region from the nonrelativistic (viz., $P_e \propto n_e^{5/3}$) to the ultrarelativistic (viz., $P_e \propto n_e^{4/3}$) regime(s), where P_e is the degenerate electron pressure and n_e is the electron number density. Dense astrophysical objects thus arise as unique cosmic laboratories for studying the properties of matter at extremely high densities (degenerate state). Naturally, in recent years, many efforts have been made to understand the properties of linear and nonlinear electrostatic waves in relativistic degenerate plasmas [8]–[12].

The dynamics of relativistic degenerate dense electron–positron–ion (e–p–i) plasma and associated collective (both linear and nonlinear) is an important area of study. Small-amplitude electrostatic pulses [10] and shocks [11] propagating in relativistic degenerate e–p–i plasmas

Manuscript received June 25, 2014; revised January 14, 2015; accepted February 9, 2015. Date of publication March 16, 2015; date of current version April 13, 2015. The work of A. ur Rahman was supported in part by the Higher Education Commission, Pakistan, within the International Research Support Initiative Program, and in part by the fellowship held at Queen's University Belfast, Belfast, U.K. The work of I. Kourakis was supported in part by the EU-FP7 IRSES Programme (FP7-PEOPLE-2013-IRSES) under Grant 612506/QUANTUM PLASMAS, and in part by the Brazilian Research Fund through the Conselho Nacional de Desenvolvimento Científico e Tecnológico—Brazil Science within the Borders Programme.

A. ur Rahman is with the Department of Physics, Islamia College Peshawar, Khyber Pakhtunkhwa, Pakistan, the Department of Physics, University of Peshawar, Peshawar 25000, Pakistan, and also with the National Centre for Physics, QAU Campus, Shahdra Valley Road, Islamabad 44000, Pakistan (e-mail: ata797@yahoo.com).

A. Qamar is with the Department of Physics, University of Peshawar, Peshawar 25000, Pakistan, and also with the National Centre for Physics, Islamabad 44000, Pakistan (e-mail: anisaqamar@gmail.com).

I. Kourakis is with the Centre for Plasma Physics, School of Mathematics and Physics, Queen's University Belfast, Belfast BT7 1NN, U.K. (e-mail: ioanniskourakissci@gmail.com).

Color versions of one or more of the figures in this paper are available online at http://ieeexplore.ieee.org.

Digital Object Identifier 10.1109/TPS.2015.2404298

were recently investigated by means of a multiscale approach. Sabry *et al.* [13] studied ion-acoustic freak waves (freak waves) in ultrarelativistic degenerate e–p–i plasmas, considering typical parameters relevant to white dwarfs and corona of magnetars. Kourakis *et al.* [14] recently explored the nonlinear dynamics of electrostatic solitary waves propagating in such plasmas, in the form of localized modulated wavepackets. They also briefly discussed the occurrence of rogue waves. More recently, McKerr *et al.* [15] considered a quantum e–p–i plasma and derived a nonlinear Schrodinger equation in their analysis. They analyzed the characteristics of different exact solutions of the nonlinear Schrödinger equation in the form of Peregrine solitons, the Akhmediev breather and the Kuznetsov–Ma breather, which are regarded as candidate functions for rogue waves.

Ion-acoustic waves, a fundamental mode in plasma environments, have been a subject of extensive research for over several decades. One of the most interesting nonlinear features of ion-acoustic waves is the existence of ion-acoustic solitary waves. There are two main approaches used to investigate ion-acoustic solitary waves, namely, the reductive perturbation technique [16] and the pseudopotential (Sagdeev) method for large-amplitude solitary waves [17]. The former method is associated with the well-known Korteweg–de Vries (KdV) equation, a paradigm widely used to model ion-acoustic solitary waves. The KdV method is valid for weak nonlinearity, so its applicability is limited to small-amplitude excitation. On the other hand, large-amplitude solitary waves may be modeled by the nonperturbative (exact) large-amplitude approach. The pseudopotential approach relies on reducing the fluid-plasma equations to an energy-integral-like equation, analogous to a classical particle subject to a potential well. The behavior of the pseudopotential is thus analyzed to predict the existence and form of the localized solitons in different plasma configurations.

Interestingly, positron production during laser–plasma interaction techniques appear to be a challenging topic recently, as ultraintense ultrashort laser pulses are made available via sophisticated technology [18], [19]. It becomes, therefore, a tempting task to investigate the effect of positrons on fundamental electrostatic modes, which is what motivates this paper that follows.

For the sake of rigor, we also mention here that in relativistic degenerate electron–positron (e–p) or e–p–i plasmas the inequality $\omega_{\mathrm{pe},p}^{-1} \ll \tau_{\mathrm{ann}}$ is assumed to be satisfied, to neglect pair annihilation effects, where $\omega_{\mathrm{pe},p}$ is the (electron and positron) plasma frequency and τ_{ann} is the annihilation time (see discussion in [10] and [20]). The process of e–p annihilation is, therefore, not taken into account in our model, for simplicity (see Appendix B).

In this paper, we study the linear and nonlinear characteristics of ion-acoustic excitations in a relativistic degenerate dense e–p–i plasma, consisting of warm nondegenerate ions and relativistic degenerate electrons and positrons. At a first step, we employ a reductive perturbation technique to derive an evolution equation in the form of a KdV equation for the electric potential and discuss its exact pulse-shaped solution. We then extend the quantum fluid model to investigate the large-amplitude nonlinear ion-acoustic waves, modeled via an energy balance-like equation involving a Sagdeev-type pseudopotential function. We establish, from first principles, the existence domains of ion-acoustic solitons in this relativistic degenerate plasmas and show how these are influenced by the electron relativistic degeneracy, the positron concentration, the ion temperature-to-electron Fermi-temperature ratio, and the soliton speed (Mach number).

This paper is arranged in the following manner. The model equations are laid out in Section II. Relying on this quantum-fluid-model, we first perform a linear analysis to obtain the dispersion characteristics of ion-acoustic waves, and then employ a reductive perturbation technique to derive a KdV equation for small-amplitude ion-acoustic excitations. Section III is devoted to arbitrary-amplitude ion-acoustic solitons, modeled using a Sagdeev pseudopotential method. In Section IV, we investigate the conditions for the existence of solitary structures. The effect of the plasma parameters relevant to our model on the characteristics of solitary waves are discussed in Section V. Finally, our results are summarized in Section VI.

II. Quantum Ion-Fluid Model

We are interested in modeling electrostatic excitations at the ionic scale propagating in an unmagnetized e–p–i plasma. For simplicity, we adopt a 1-D geometry. The ions are assumed to constitute a system of warm particles with an individual charge of $Z_i e$ (Z_i denotes the ion charge state, while e is the electron charge), subject to the influence of the electrostatic potential ϕ, while the electrons and positrons are considered as a relativistically degenerate ensemble, following the Fermi–Dirac formalism.

Adopting a 1-D fluid formulation, the evolution equations for the ion density n_i, fluid speed v_i, and electron/positron pressure $P_{e/p}$ read

$$\frac{\partial n_i}{\partial t} + \frac{\partial}{\partial x}(n_i v_i) = 0 \tag{1}$$

$$\frac{\partial v_i}{\partial t} + v_i \frac{\partial v_i}{\partial x} + \frac{Z_i e}{m_i}\frac{\partial \phi}{\partial x} + \frac{1}{m_i n_i}\frac{\partial P_i}{\partial x} = 0 \tag{2}$$

$$e n_e \frac{\partial \phi}{\partial x} - \frac{\partial P_e}{\partial x} = 0 \tag{3}$$

$$e n_p \frac{\partial \phi}{\partial x} + \frac{\partial P_p}{\partial x} = 0 \tag{4}$$

$$\frac{\partial^2 \phi}{\partial x^2} = 4\pi e(n_e - Z_i n_i - n_p) \tag{5}$$

where n_e, n_p, and m_i represent the electron density, positron density, and ion mass, respectively. We shall adopt (for electrons and positrons, respectively, denoted by the subscript $j = e, p$) the relativistic Chandrasekhar EoS [6], [7]

$$P_j = \frac{\pi m_j^4 c^5}{3h^3}\left[\eta_j\left(2\eta_j^2 - 3\right)\left(1+\eta_j^2\right)^{\frac{1}{2}} + 3\sinh^{-1}(\eta_j)\right] \tag{6}$$

where $\eta_j = p_{Fj}/m_j c = (\gamma_j^2 - 1)^{1/2}$, while $p_{Fj} = (2m_j E_{Fj})^{1/2} = (3h^3 n_j/8\pi)^{1/3}$ is the Fermi momentum and $\gamma_j = (1+\eta_j^2)^{1/2}$, while $\sinh^{-1}$ denotes the inverse hyperbolic sine function.

Charge neutrality at equilibrium imposes the condition $n_{e0} = Z_i n_{i0} + n_{p0}$, where n_{s0} denotes the number density of the sth species ($s = e,\ p,\ i$ henceforth standing for electrons, positrons, and ions, respectively).

Equations (3) and (4) can be integrated as

$$\frac{1}{n_j}\frac{\partial P_j}{\partial x} = \frac{m_j c^2 \eta_j}{\left(1+\eta_j^2\right)^{\frac{1}{2}}}\frac{\partial \eta_j}{\partial x}.$$

The number densities can then be expressed as functions of ϕ

$$n_j = \frac{8\pi m_j^3 c^3}{3h^3}\left[\frac{e^2\phi^2}{m_j^2 c^4} \pm \frac{2e\phi}{m_j c^2}\left(1+\eta_{j0}^2\right)^{\frac{1}{2}} + \eta_{j0}^2\right]^{\frac{3}{2}} \quad (7)$$

and therefore reduce the number of equations to three. In (7), $\eta_{j0} = (3h^3 n_{j0}/8\pi m^3 c^3)^{1/3}$ is the value of the relativity parameter, η_j, at equilibrium. In (7), the positive sign is taken into account for electrons ($j = e$) and the $-$ sign for positrons ($j = p$). The detailed derivation of (7) is provided in Appendix A.

A. Scaled Evolution Equations

For analytical convenience, we have cast the dynamical evolution equations in a dimensionless form, by making use of the following normalization. Space (x) and time (t) are scaled by C_i/ω_{pi} and $\omega_{pi}^{-1} = (m_i/4\pi n_{i0} Z_i^2 e^2)^{1/2}$, respectively, while the electrostatic potential is scaled by $\phi_0 = (E_{\mathrm{Fe}0}/Z_i e)$, the ion fluid speed by $C_i = (E_{\mathrm{Fe}0}/m_i)^{1/2}$ and the number density n_s by n_{s0}. We have defined the quantities: $p = (n_{p0}/n_{e0})$, $g_i = 3T_i/T_{\mathrm{Fe}0}$, which, respectively, represent the ratio of positron density to electron density and the ratio of ion temperature to electron Fermi temperature. We have defined the ratios

$$\frac{n_{e_0}}{Z_i n_{i0}} = \frac{1}{1-p}, \quad \frac{n_{p0}}{Z_i n_{i0}} = \frac{p}{1-p}$$

and also $T_{\mathrm{Fe}0} = (\hbar^2/2m_e k_B)(3\pi^2 n_{e0})^{2/3}$, where $\hbar$ is the reduced Planck constant and k_B being the Boltzmann constant. The ratio $g_i = 3T_i/T_{\mathrm{Fe}0}$, which acquires very small values, accounts for thermal effects.

By employing a Taylor series, we expand (5) up to second order, and the following normalized system of fluid equations are obtained:

$$\frac{\partial \tilde{n}_i}{\partial \tilde{t}} + \frac{\partial}{\partial \tilde{x}}(\tilde{n}_i \tilde{v}_i) = 0 \quad (8)$$

$$\frac{\partial \tilde{v}_i}{\partial \tilde{t}} + \tilde{v}_i\frac{\partial \tilde{v}_i}{\partial \tilde{x}} + \frac{\partial \tilde{\phi}}{\partial \tilde{x}} + g_i\tilde{n}_i\frac{\partial \tilde{n}_i}{\partial \tilde{x}} = 0 \quad (9)$$

$$\frac{\partial^2 \tilde{\phi}}{\partial \tilde{x}^2} + (\tilde{n}_i - 1) \simeq c_1\tilde{\phi} + c_2\tilde{\phi}^2 \quad (10)$$

where the coefficients (containing all the information regarding the plasma configuration) in the right-hand side are defined as

$$c_1 = \frac{3\gamma_{e0}}{2(1-p)} + \frac{3pE_{\mathrm{Fe}0}\gamma_{p0}}{2E_{Fp0}(1-p)} \quad (11)$$

and

$$c_2 = \frac{3}{8(1-p)}\left(2\gamma_{e0}^2 - 1\right) - \frac{3pE_{\mathrm{Fe}0}^2}{8E_{Fp0}^2(1-p)}\left(2\gamma_{p0}^2 - 1\right) \quad (12)$$

where $E_{Fj0} = mc^2\eta_{j0}^2/2$ and $\gamma_{j0} = (1+\eta_{j0}^2)^{1/2}$.

For the remainder of this paper, the scaled variables will be used (dropping the tilde where obvious). Moreover, η_j is defined as $\eta_j = (n_j/n_0)^{1/3}$, in which $n_0 = (8\pi m^3 c^3/3h^3) \approx 5.9 \times 10^{29}$ cm^{-3}. For electrons $\eta_{e0} = (n_{e0}/n_0)^{1/3}$, which is also known as the electron relativistic degeneracy parameter. The positron relativistic degeneracy parameter η_{p0}, can be expressed in terms of η_{e0} as, $\eta_{p0} = p^{1/3}\eta_{e0}$.

B. Linear Analysis

Linearizing the above system of fluid model equations, and then Fourier analyzing in terms of the normalized wave number k and angular wave frequency ω, a linear dispersion relation is obtained in the form

$$\frac{\omega^2}{k^2} = \frac{1}{c_1 + k^2} + g_i. \quad (13)$$

A few comments regarding the latter (dispersion) relation (13) are in order. First, for $k \ll \sqrt{c_1}$ (i.e., in the long wavelength limit), the ion-acoustic phase speed reads

$$\frac{\omega}{k} \simeq \left(\frac{1}{c_1} + g_i\right)^{\frac{1}{2}} \quad (14)$$

which shows how the phase speed is strongly influenced by the positron to electron density ratio and the relativistic degeneracy parameter (via c_1) and ion temperature to electron Fermi temperature ratio (via g_i). On the other hand, in the opposite case, i.e., for a very short wavelength limit, $v_{\mathrm{ph}}(\sim\omega/k) \to g_i$, hence the (ion) thermal contributions become dominant at high wavenumbers. Restoring the dimensions for a while, one can find from (13) the effective charge screening length, which is given by

$$\lambda_{Fi}^{(R)} = c_1^{\frac{-1}{2}}\lambda_{Fi}. \quad (15)$$

It is straightforward to see that $\lambda_{Fi}^{(R)}$ is reduced with the positron concentration (p) and with the relativity parameter (η_{e0}).

In Fig. 1, we have displayed the dispersion curves of ion-acoustic mode for various values of intrinsic relevant plasma parameters, i.e., of the electron relativistic degeneracy parameter η_{e0}, the positron to electron density ratio, p, and the ion temperature to electron Fermi temperature ratio, g_i. It is evident that the angular frequency ω decreases with an increase in the relativity parameter η_{e0}, and a significant reduction is observed in ω for higher values of p [Fig. 1(b)]. By looking at Fig. 1(c), it is clear that ω increases as g_i increases, but this effect is prominent at higher values of the wave number k. Consequently, the phase speed decreases as η_{e0} or p increases, while increasing values of g_i gives enhanced ion-acoustic phase speed.

C. KdV Theory for Weak-Amplitude Pulse Excitations

We shall now investigate the small (but finite) amplitude regime, beyond the linear approximation. A variable transformation is adopted as [16]

$$\zeta = \epsilon^{\frac{1}{2}}(x - Vt) \quad \text{and} \quad \tau = \epsilon^{\frac{3}{2}}t \quad (16)$$

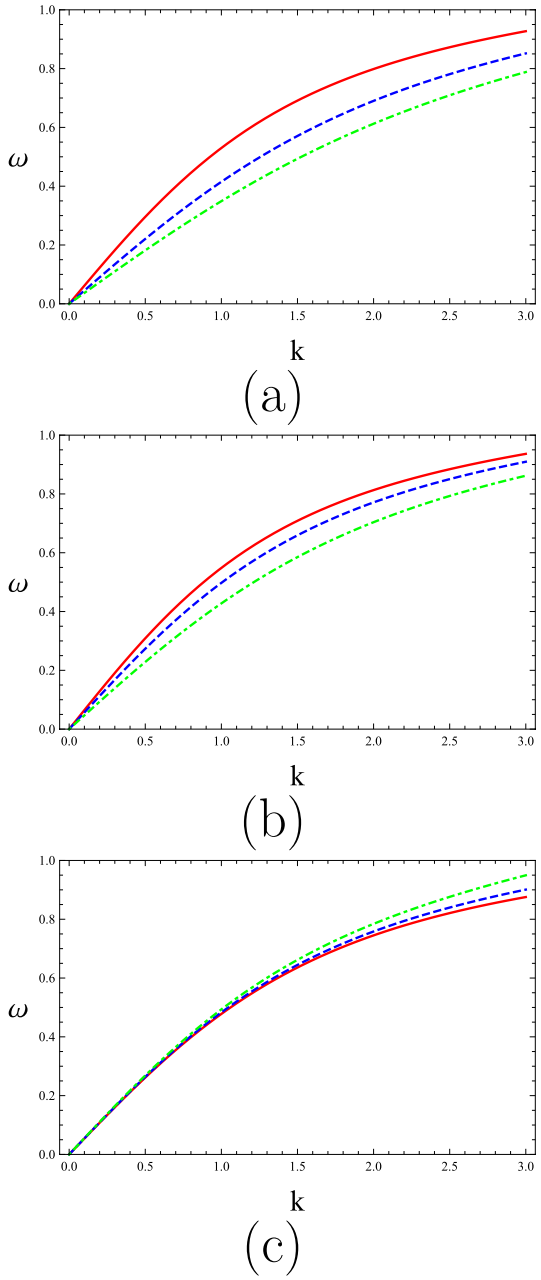

Fig. 1. Plot of the dispersion relation relating the frequency ω to the wave number k. (a) ω versus k for different values of p. Solid curve: $p = 0.01$; dashed curve: $p = 0.3$; and dotted-dashed curve: $p = 0.5$. Here, $g_i = 0.01$ and $\eta_{e0} = 1.19$. (b) ω versus k for different η_{e0}. Solid curve: $\eta_{e0} = 0.01$; dashed curve: $\eta_{e0} = 1$; and dotted-dashed curve: $\eta_{e0} = 2$, where $p = 0.1$ and $g_i = 0.01$. (c) ω versus k for different values of g_i. Solid curve: $g_i = 0.005$; dashed curve: $g_i = 0.01$; and dotted-dashed curve: $g_i = 0.02$. Here, $p = 0.1$ and $\eta_{e0} = 1.19$.

where ϵ $(0 < \epsilon \ll 1)$ is a small dimensionless parameter that measures the weakness of the nonlinearity, and V is the normalized wave phase speed (to be determined later). We also expand the dependent variables n_s, ϕ, and u_i near their unperturbed values in power series of ϵ as

$$\begin{aligned} n_s &= 1 + \epsilon n_{s1} + \epsilon^2 n_{s2} + \cdots \\ \phi &= 0 + \epsilon \phi_1 + \epsilon^2 \phi_2 + \cdots \\ u_i &= 0 + \epsilon u_{i1} + \epsilon^2 u_{i2} + \cdots \end{aligned} \tag{17}$$

Substituting (16) and (17) into (9), the lowest orders in ϵ $(\sim \epsilon^{1/2})$ give

$$n_{i1} = \frac{1}{V^2}\phi_1 \quad \text{and} \quad u_{i1} = \frac{\phi_1}{V}. \tag{18}$$

Using (18), along with the lowest order in ϵ of Poisson's equation eventually gives

$$V = \left(g_i + \frac{1}{c_1}\right)^{\frac{1}{2}}. \tag{19}$$

The latter equation identifies the soliton speed as the sound speed (acoustic speed) defined in (14). The above expression outlines the fact that the ion-acoustic soliton speed is significantly affected by the electron relativistic degeneracy parameter (via η_{e0}), the positron to electron density ratio (via p), and the ion temperature to electron Fermi temperature ratio (via g_i). Now next orders in ϵ, give a system of equations containing second-order perturbed quantities (n_{i2}, u_{i2}, and ϕ_2). Solving this system of equations with the aid of (18) and (19), we finally obtain an evolution equation for the electric potential disturbance ϕ_1, in the form of KdV equation

$$\frac{\partial \phi_1}{\partial \tau} + A\phi_1 \frac{\partial \phi_1}{\partial \zeta} + B\frac{\partial^3 \phi_1}{\partial \zeta^3} = 0. \tag{20}$$

The second term represents the nonlinearity (responsible for wave steepening), and the third term corresponds to the dispersion (causing wave broadening), and their associated coefficients are defined as

$$A = B\left(\frac{3V^2 + g_i}{(V^2 - g_i)^3} - 2c_2\right) \tag{21}$$

and

$$B = \frac{(V^2 - g_i)^2}{2V}. \tag{22}$$

To get the stationary solitary wave solution of (20), we introduce the transformation $\chi = \zeta - U_0\tau = \epsilon^{1/2}\{x - (V + \epsilon U_0)t\}$, where U_0 (normalized by C_i) is a constant speed of a solitary structure representing the velocity increment above the linear phase speed V. By applying the vanishing boundary conditions: $\phi_1 \to 0$, $d\phi_1/d\chi \to 0$, and $d^2\phi_1/d\chi^2 \to 0$ at $|\chi| \to \infty$, we obtain

$$\frac{1}{2}\left(\frac{d\phi_1}{d\chi}\right)^2 = \frac{U_0}{2B}\phi_1^2 - \frac{A}{6B}\phi_1^3 \tag{23}$$

which can be further solved to obtain the solitary wave solution of the form [21], as

$$\phi_1 = \phi_m \operatorname{sech}^2\left(\frac{\zeta - U_0\tau}{\Delta}\right) \tag{24}$$

where ϕ_m and Δ are, respectively, the maximum amplitude and width of the localized pulse. The parameters ϕ_m and Δ are defined as

$$\phi_m = \frac{3U_0}{A} \text{ and } \Delta = \left(\frac{4B}{U_0}\right)^{\frac{1}{2}} \tag{25}$$

satisfying the relation $\phi_m \Delta^2 = 12B/A$. Note that the amplitude (width) of the solitons increases (decreases, respectively) with U_0, suggesting that faster solitons will be taller and narrower, whereas slower ones will be shorter and wider.

III. Sagdeev Pseudopotential Method

The analysis carried out in the previous section dealt with small-amplitude weakly super-acoustic electrostatic solitary waves. In this section, we relax those constraints by considering arbitrary amplitude nonlinear ion-acoustic excitations.

In anticipation of stationary-profile excitations, we shall assume that all the fluid variables in the evolution equations depend on the single variable $\chi = x - Mt$, where χ is a new (moving) space variable normalized by C_i/ω_{pi}, while M will be referred to as the Mach number, viz., the soliton speed, scaled by C_i (analogous to the sound speed in classical plasmas). Incorporating the transformation into the above system of fluid equations leads to

$$-M\frac{dn_i}{d\chi} + \frac{d}{d\chi}(n_i u_i) = 0 \tag{26}$$

$$-M\frac{du_i}{d\chi} + u_i\frac{du_i}{d\chi} + \frac{d\phi}{d\chi} + g_i n_i \frac{\partial n_i}{\partial \chi} = 0 \tag{27}$$

$$\frac{d^2\phi}{d\chi^2} = \beta n_e - \alpha n_p - n_i. \tag{28}$$

Integrating (26) and (27), and imposing the appropriate boundary conditions for localized waves ($n_i \to 1$, $u_i \to 0$, and $\phi \to 0$ as $\chi \to \pm\infty$), we find

$$u_i = M\left(1 - \frac{1}{n_i}\right) \tag{29}$$

and

$$g_i n_i^4 - (M^2 + g_i - 2\phi)n_i^2 + M^2 = 0. \tag{30}$$

Equation (30) is quadratic in n_i^2 and can be solved as

$$n_i^2 = \frac{(M + g_i - 2\phi) \pm \sqrt{(M + g_i - 2\phi)^2 - 4M^2 g_i}}{2g_i}. \tag{31}$$

To find a solution of (31) for n_i, we follow the idea of [22], by assuming a solution in the form

$$n_i = \frac{1}{\sqrt{2}}\left(\sqrt{p} \pm \sqrt{q}\right)$$

where p and q are real quantities, to be determined. Squaring the above expression and comparing the resulting terms with (31), we find, eventually

$$n_i = \frac{1}{2\sqrt{g_i}}\left\{\left[(M+\sqrt{g_i})^2 - 2\phi\right]^{\frac{1}{2}} - \left[(M - \sqrt{g_i})^2 - 2\phi\right]^{\frac{1}{2}}\right\}. \tag{32}$$

We note that one of the roots in (31) has been excluded, as it failed to satisfy the explicit boundary condition (requirement), namely, that $n_i = 1$ at $\phi = 0$. Here, we have assumed that: 1) $M > \sqrt{g_i}$ and 2) $\phi \leq (M - \sqrt{g_i})^2/2 \equiv \phi_{\max}$ (which ensures the reality of n_i). We note that, upon setting $g_i \to 0$, the cold-ion limit is recovered

$$n_i = \left(1 - \frac{2\phi}{M^2}\right)^{\frac{-1}{2}}. \tag{33}$$

The number density of electrons and positrons in terms of electrostatic potential can be expressed as [see (7)]

$$n_e = \eta_{e0}^{-3}\left[\eta_{e0}^2 + \phi\left(2\sqrt{1 + \eta_{e0}^2} + \phi\right)\right]^{\frac{3}{2}} \tag{34}$$

$$n_p = p^{-1}\eta_{e0}^{-3}\left[p^{\frac{2}{3}}\eta_{e0}^2 - \phi\left(2\sqrt{1 + p^{\frac{2}{3}}\eta_{e0}^2} - \phi\right)\right]^{\frac{3}{2}}. \tag{35}$$

Substituting (32)–(35) into (28), multiplying the resulting equation by $d\phi/d\chi$, integrating once, and imposing the appropriate boundary conditions for localized solutions, namely, $\phi \to 0$, $d\phi/d\chi \to 0$ at $\chi \to \pm\infty$, one obtains the integral equation as

$$\frac{1}{2}\left(\frac{d\phi}{d\chi}\right)^2 + V(\phi) = 0 \tag{36}$$

mimicking a pseudomechanical energy balance equation, where $V(\phi)$ is the Sagdeev-type pseudopotential [17].

Here, $P(\phi) = \eta_{e0}^2 + \phi(\phi + 2(1 + \eta_{e0}^2)^{1/2}$ and $Q(\phi) = \eta_{p0}^2 + \phi(\phi - 2(1 + \eta_{p0}^2)^{1/2})$. Equation (36) can be regarded as an energy integral of particle of unit mass, with pseudospeed $d\phi/d\chi$, pseudotime χ, pseudoposition ϕ, and pseudopotential $V(\phi)$. Obviously, the motion is restricted to the negative $V(\phi)$ region. In deriving (37), as shown at the bottom of this page, the boundary conditions ϕ, $d\phi/d\chi \to 0$ as $\chi \to \pm\infty$ have been used.

A. Small Amplitude Weakly Super-Acoustic Limit of the Sagdeev Equation

In this section, we shall establish the equivalence between the KdV theory (valid near the sound speed) and the Sagdeev theory. By setting $M \simeq V + U_0$ (where $U_0 \ll V$) and Taylor expanding the Sagdeev potential up to third order in ϕ (assuming $\phi \ll 1$), so that (37) takes the following approximate form:

$$V(\phi) \approx a\phi^2 + b\phi^3 \tag{38}$$

where

$$a = \frac{VU_0}{\left(V^2 - g_i\right)^2} \tag{39}$$

and

$$b = \frac{1}{6}\left[\frac{3V^2 + g_i}{\left(V^2 - g_i\right)^3} - 2c_2\right]. \tag{40}$$

$$\begin{aligned} V(\phi) = {} & (6\sqrt{g_i})^{-1}\left\{\left[(M - \sqrt{g_i})^2 - 2\phi\right]^{\frac{3}{2}} - \left[(M + \sqrt{g_i})^2 - 2\phi\right]^{\frac{3}{2}} - (M - \sqrt{g_i})^3 + (M + \sqrt{g_i})^3\right\} \\ & + \left(8(1-p)\eta_{e0}^3\right)^{-1}\Big\{-3\eta_{e0}\left(\gamma_{e0} + p^{\frac{1}{3}}\gamma_{p0}\right) - 2P(\phi)\eta_{e0}^2(3\phi + \gamma_{e0}) - P(\phi)\left(\phi + 2\phi^3 - 3\gamma_{e0} + 6\phi^2\gamma_{e0}\right) \\ & + 2\eta_{e0}^3(\gamma_{e0} + p\gamma_{p0}) - 2Q(\phi)p^{\frac{2}{3}}\eta_{e0}^2(-3\phi + \gamma_{p0}) + Q(\phi)\left(\phi + 2\phi^3 + 3\gamma_{p0} - 6\phi^2\gamma_{p0}\right) \\ & - 3\ln\left(p^{\frac{1}{3}}\eta_{e0} - \gamma_{p0}\right) + 3\left(\sinh^{-1}(\eta_{e0}) - \ln[\phi + \gamma_{e0} + P(\phi)]\right) + 3\ln[\phi - \gamma_{p0} + Q(\phi)]\Big\}. \end{aligned} \tag{37}$$

Equation (36) thus becomes

$$\frac{1}{2}\left(\frac{d\phi}{d\chi}\right)^2 + a\phi^2 + b\phi^3 = 0. \quad (41)$$

Clearly, the coefficients of ϕ^2 and ϕ^3 in the above expression are the same as in (23), noting that $a = U_0/2B$ and $b = A/6B$.

We conclude that the small amplitude expansion of the Sagdeev energy balance equation gives exactly the same result as predicted by the KdV theory, for pulses moving at a weakly supersonic velocity.

IV. Ion-Acoustic Solitary Waves: Existence Conditions

Stationary-profile excitations can now be obtained from (36) and (37), via numerical integration. It is instructive to discuss the conditions under which (36) leads to soliton solutions by analyzing the Sagdeev potential (37). It is clear from (37) that $V(\phi)$ and $dV(\phi)/d\phi = 0$ at $\phi = 0$. Solitary wave solutions of (36) exist if: 1) $d^2V(\phi)/d\phi^2 < 0$ at $\phi = 0$, so that the fixed point at the origin is unstable; 2) there exists a nonzero ϕ_m at which $V(\phi_m) = 0$; and 3) $V(\phi) < 0$ when ϕ lies between 0 and ϕ_m. It is of interest to determine the lower and upper limits of the Mach number M for which solitons exist. Applying 1), we obtain

$$M > \left[\frac{(1-p)\eta_{e0}^2}{3\eta_{e0}\left(\gamma_{e0}+p^{\frac{1}{3}}\gamma_{p0}\right)}+g_i\right]^{\frac{1}{2}} = \left(\frac{1}{c_1}+g_i\right)^{\frac{1}{2}} \equiv M_1 \quad (42)$$

which is the lower limit for M, corresponding exactly to the true normalized ion-acoustic phase speed as given by (19). Hence, M_1 is the real sound speed [in agreement with (14)] and the solitons will be supersonic (super acoustic) as expected. Our results are quite interesting in regard that it fit with literature regarding the physical interpretation of KdV which meant to be weakly super acoustic. In the absence of positrons and for cold-ion limit (i.e., by setting $g_i = 0$ and $p = 0$), we recover the earlier result of [12, eq. (14)]. Moreover, by taking $p = 1$, we have a pure e–p plasma, in which case ion acoustic waves cannot be supported. It can be easily seen from (42) that the lower Mach number limit M_1 increases with g_i and decreases for higher values of η_{e0} and p, showing that the sound speed is reduced, in comparison with electron–ion plasma.

The reality of n_i, given by (32), implies that $\phi < \phi_m = (M-\sqrt{g_i})^2/2$ assuming positive pulses. In combination with 2) and 3) above, this imposes the condition $V(\phi_m) \geq 0$, which leads to the following equation for the upper limit in M:

$$\begin{aligned}
&\delta - \frac{3\gamma_{e0}}{8\eta_{e0}^2(1-p)} - \frac{3p^{\frac{1}{3}}\gamma_{p0}}{8\eta_{e0}^2(1-p)} + \frac{\gamma_{e0}+p\gamma_{p0}}{4(1-p)} \\
&+\frac{\eta_{p0}^2 R(-2\gamma_{p0}+3T^2)}{16\eta_{e0}^3(1-p)} + \frac{R[12\gamma_{p0}+(2+(-6\gamma_{p0}+T)T)T]}{64\eta_{e0}^3(1-p)} \\
&-\frac{S(2\gamma_{e0}+3T)}{16\eta_{e0}(1-p)} - \frac{S(-12\gamma_{e0}+2T+6\gamma_{e0}T^2+T^3)}{64\eta_{e0}^3(1-p)} \\
&+\frac{3(\sinh^{-1}[\eta_{e0}] - \ln[\gamma_{e0}+(S/2)+(T/2)])}{8\eta_{e0}^3(1-p)} \\
&-\frac{(-\ln[\eta_{p0}-\gamma_{p0}]+\ln[-\gamma_{p0}+(R/2)+(T/2)])}{8\eta_{e0}^3(1-p)} = 0 \quad (43)
\end{aligned}$$

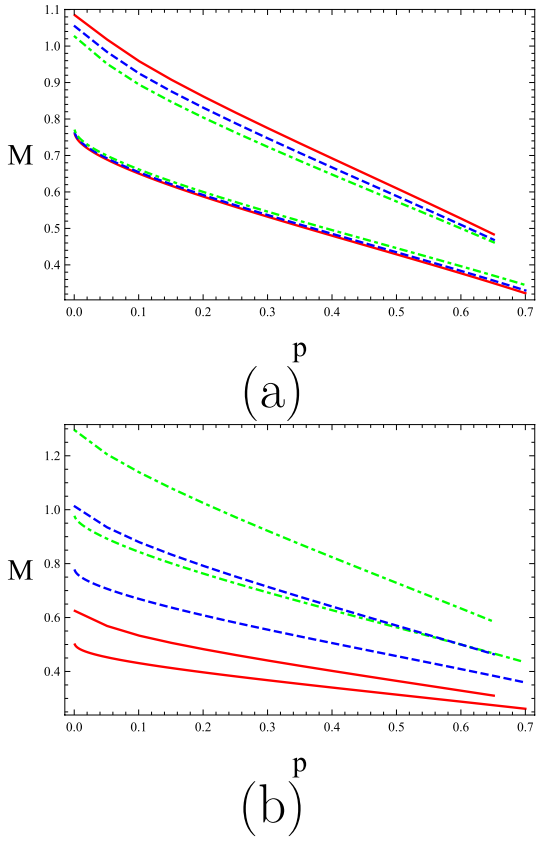

Fig. 2. Minimum and maximum Mach numbers $[M_1, M_2]$ are depicted versus p (positron content), for different values of (a) ion temperature ratio g_i and (b) electron relativistic degeneracy parameter η_{e0}. The lower curves in the respective style(s) (solid, dashed, and dotted-dashed) represent the lower limit M_1, while the upper curves in the corresponding style give the upper limit M_2. Solitons may exist for values of the Mach number in the region between the lower and upper curves of the same color/style. (a) Solid curves: $g_i = 0.005$; dashed curves: $g_i = 0.01$; and dotted-dashed curves: $g_i = 0.03$. Here, $\eta_{e0} = 2$. (b) Solid curves: $\eta_{e0} = 1$; dashed curves: $\eta_{e0} = 2$; and dotted-dashed curves: $\eta_{e0} = 3$, where $g_i = 0.03$.

where $\delta = 1/3(3M^2 - M^{3/2}g_i^{1/4} + g_i)$, $S = (4\eta_{e0}^2 + 4\gamma_{e0}T + T^2)^{1/2}$, $R = (4\eta_{p0}^2 + (-4\gamma_{p0}+T)+T)^{1/2}$, and $T = (M-\sqrt{g_i})^2$. Solving (43) numerically gives the upper limit M_2 for solitons to exist. We note here for comparison that in the limiting case, where $g_i \to 0$ and $p \to 0$, the above constraint (43) reduces to the one already derived in [12].

Ion-acoustic potential excitations occur for values of M in the region $M_1 < M < M_2$. Both these constraints vary with the intrinsic parameters relevant to our model, namely, η_{e0}, p, and g_i. Therefore, it is essential to study their dependence on these physical parameters. We have taken $Z_i = 1$ for simplicity in the following. The results have been displayed in Figs. 2 and 3.

In Fig. 2, we have shown the range of allowed Mach numbers for ion acoustic solitary waves with p, for various values of η_{e0} and g_i. The lower curves correspond to the lower limit M_1 found by evaluation of the analytically derived relation (42), while the upper curves give the upper limit M_2, obtained via numerical solution of (43). Interestingly, we see that the soliton existence region shrinks, as the curves approach each other slightly for higher values of g_i [Fig. 2(a)]. Further, we also note that increasing values of p makes the ion

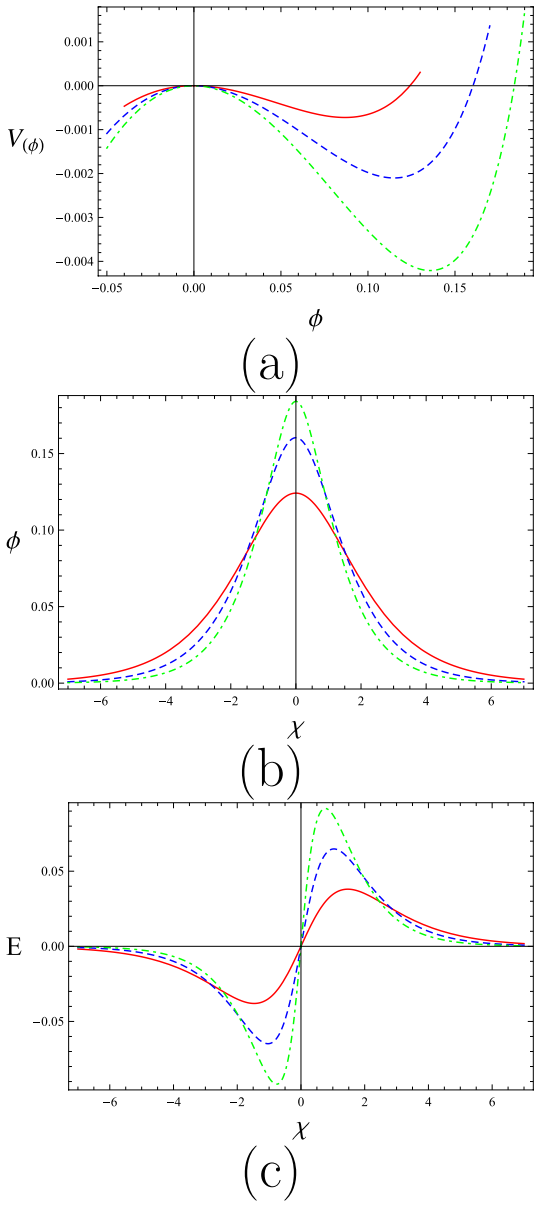

Fig. 3. Variation of (a) $V(\phi)$ versus ϕ, (b) ion-acoustic solitary wave profiles ϕ versus χ, and (c) electric field E versus χ, for different values of the positron concentration p. The solid curves correspond to $p = 0.05$; dashed curves to $p = 0.1$; and dotted-dashed curves to $p = 0.15$. Other parameters are $g_i = 0.03$, $M = 0.8$, and $\eta_{e0} = 2$.

acoustic solitary pulses slower, i.e., the allowed Mach number domain $[M_1, M_2]$ acquires lower values for higher values of p. Significant dependence of the soliton existence domain $[M_1, M_2]$ on η_{e0} is shown in Fig. 2(b) for various values of η_{e0}, while keeping values of p and g_i fixed. We thus observe that both M_1 and M_2, i.e., the entire soliton existence domain, shift(s) higher upon increasing values of $\eta_{e0}(= 1, 2, 3)$. This is in agreement with earlier result found in [12].

V. Ion-Acoustic Solitary Waves: Form and Characteristics

We shall now discuss the configurational characteristics of solitary waves (amplitude and width), relying on the

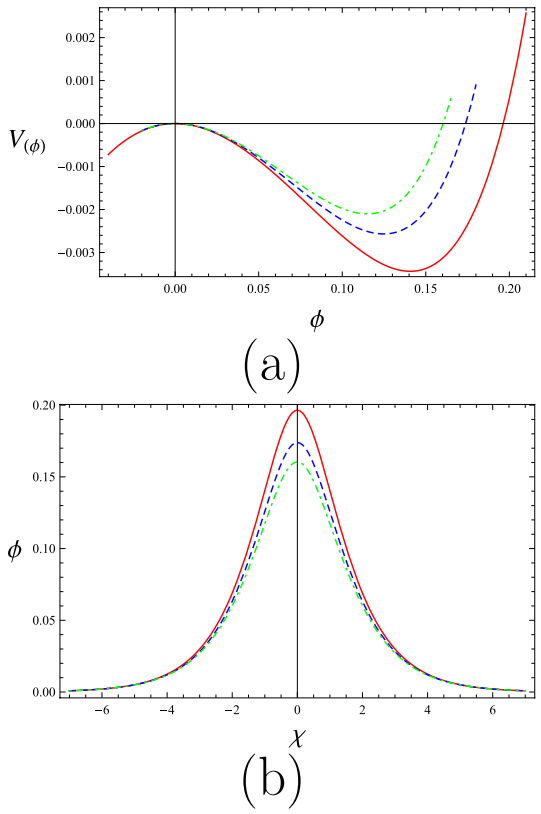

Fig. 4. Variation of (a) $V(\phi)$ versus ϕ and (b) associated solitary wave profiles ϕ versus χ, for different values of the ion temperature ratio g_i. Solid curve: $g_i = 0.005$; dashed curve: $g_i = 0.02$; and dotted-dashed curve: $g_i = 0.03$. Here, $p = 0.1$, $M = 0.8$, and $\eta_{e0} = 2$.

Sagdeev pseudopotential approach outlined above. We have numerically solved (36) in combination with (37) for different parameter values relevant to our model, to examine their effect on the form and characteristics of ion-acoustic solitary waves. The results are displayed in Figs. 3–7. The plots provided here are based on parameter values characteristic of relativistic degenerate plasmas found in dense astrophysical objects, such as in white dwarfs etc., where the typical interior densities are $\rho \simeq 10^6$ g/cm^{-3} [1], [4].

A. Positron Content Effect

To examine the effect of p on the soliton characteristics, we depict the variation of $V(\phi)$, of the solitary wave (solution) profile and of the associated ambipolar electric field structure E (obtained numerically) with p (for fixed values of η_{e0}, g_i, and M). We observe that the solitary wave amplitude increases monotonically for increasing values of $p(= 0.05, 0.1, 0.2)$ [Fig. 3(a)]. It is also seen that the depth of the Sagdeev potential increases with increasing values of p. Recalling that the depth of Sagdeev potential is related to the maximum value of $\phi'(\chi)$ through (36), we deduce that a deeper potential well refers to (steeper) narrower solitary waves. The amplitude (width) of the associated solitary profiles [Fig. 3(b)] is found to increase (decrease) with increasing values of p. A similar variation of the bipolar electric field structures is shown in Fig. 3(c) for higher values of p.

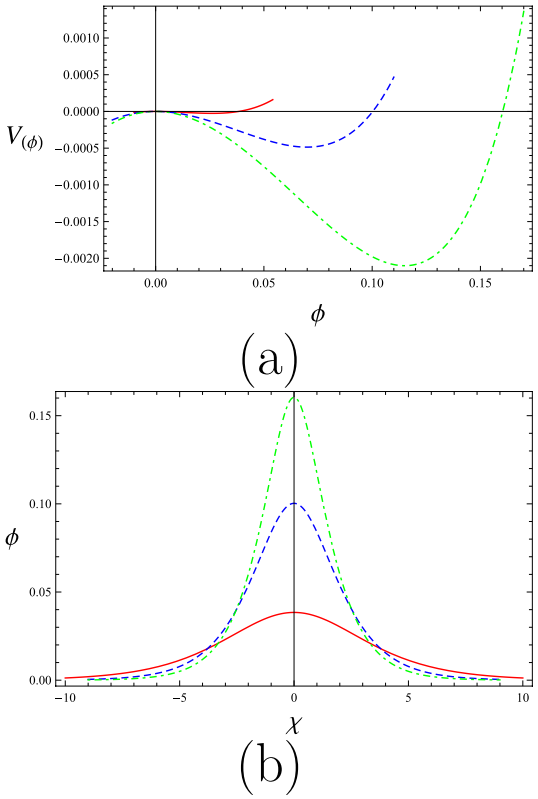

Fig. 5. Variation of (a) $V(\phi)$ versus ϕ and (b) corresponding solitary wave profiles ϕ versus χ, for different values of the Mach number M. Solid curve: $M = 0.7$; dashed curve: $M = 0.75$; and dotted-dashed curve: $M = 0.8$. Here, $p = 0.1$, $g_i = 0.03$, and $\eta_{e0} = 2$.

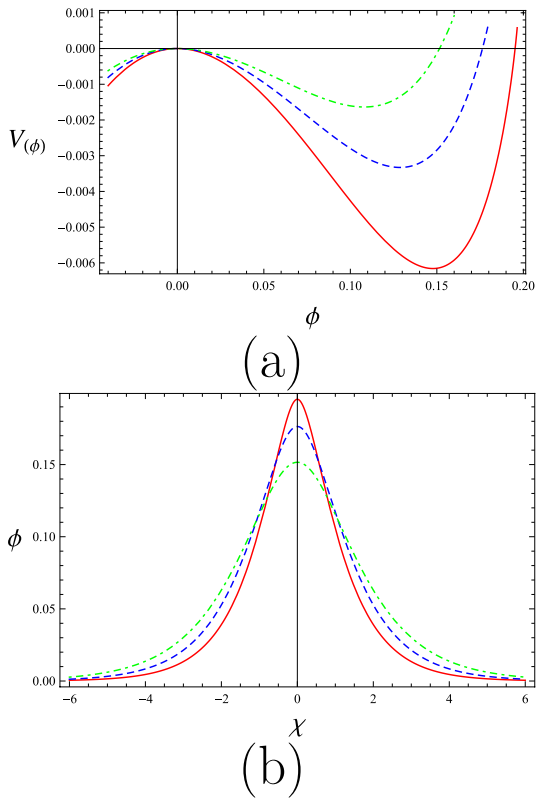

Fig. 6. Variation of (a) $V(\phi)$ versus ϕ and (b) associated solitary wave profiles ϕ versus χ, for various values of the electron relativistic degeneracy parameter η_{e0}. Solid curve: $\eta_{e0} = 1.75$; dashed curve: $\eta_{e0} = 1.90$; and dotted-dashed curve: $\eta_{e0} = 2.05$. Here, $p = 0.1$, $g_i = 0.03$, and $M = 0.8$.

B. Ion Thermal Effect

In Fig. 4, we show the variation of the pseudopotential $V(\phi)$ and of the corresponding solitary wave structures $\phi(\chi)$ for different values of g_i, while keeping η_{e0} and p fixed. It is seen clearly from Fig. 4 that increasing the value of g_i leads to a reduction of the depth of Sagdeev potential and, importantly, also of the amplitude of the associated ion-acoustic solitary wave. We see that including the finite ion temperature effect (in the warm ion model) gives rise to dispersive effects, which tend to suppress the effects due to nonlinearity, resulting in smaller amplitudes of ion-acoustic solitary waves.

C. Pulse Speed Effect

To express the effect of the soliton speed (Mach number M) on the localized solutions (solitary waves), we have depicted the pseudopotential $V(\phi)$ and the associated solutions $\phi(\chi)$ for various values of M chosen within the range $M\epsilon[M_1, M_2]$, in Fig. 5. It is seen that, with increasing values of M, ion-acoustic solitons with higher amplitude and reduced width are obtained. This result qualitatively agrees with the KdV picture, suggesting that faster solitons will be taller and steeper.

D. Relativistic Degeneracy Effect

Fig. 6 manifests the fact that the shape of soliton changes with η_{e0}. It is shown that increasing the values of $\eta_{e0}(=1.75, 1.90, 2.05)$ leads to deeper pseudopotential curves, and also to a decrease in the amplitude of the resulting solitary waves, as shown in Fig. 6(b).

E. Maximum Electrostatic Potential Pulse Amplitude

It is interesting to mention that in the Sagdeev approach employed above, the soliton amplitude [viz., root of $V(\phi)$] is determined as the root of the pseudopotential function, i.e., by numerically solving $V(\phi_m) = 0$. Fig. 7 shows how the soliton amplitude ϕ_m varies with p, g_i, M, and η_{e0}. It is seen that ϕ_m decreases with η_{e0} suggesting that assuming higher values of the relativistic degeneracy parameter suppresses the pulse strength. The dependence on ion thermal effects (via the temperature ratio g_i) is qualitatively similar, though less dramatic.

Interestingly, the soliton amplitude (maximum value) is an increasing function of (the positron content) p, suggesting that positrons enhance and stabilize localized electrostatic disturbances.

Finally, as expected from similar works on classical plasmas, the maximum value of the electrostatic potential is also an increasing function of the propagation speed M. This reflects our earlier results appearing in Figs. 3–6, leading to the conclusion that the soliton amplitude gets amplified with higher values of p and M, and diminishes with increased values of g_i and η_{e0}.

The above results on the characteristics of ion-acoustic solitary waves are graphically summarized in Fig. 7.

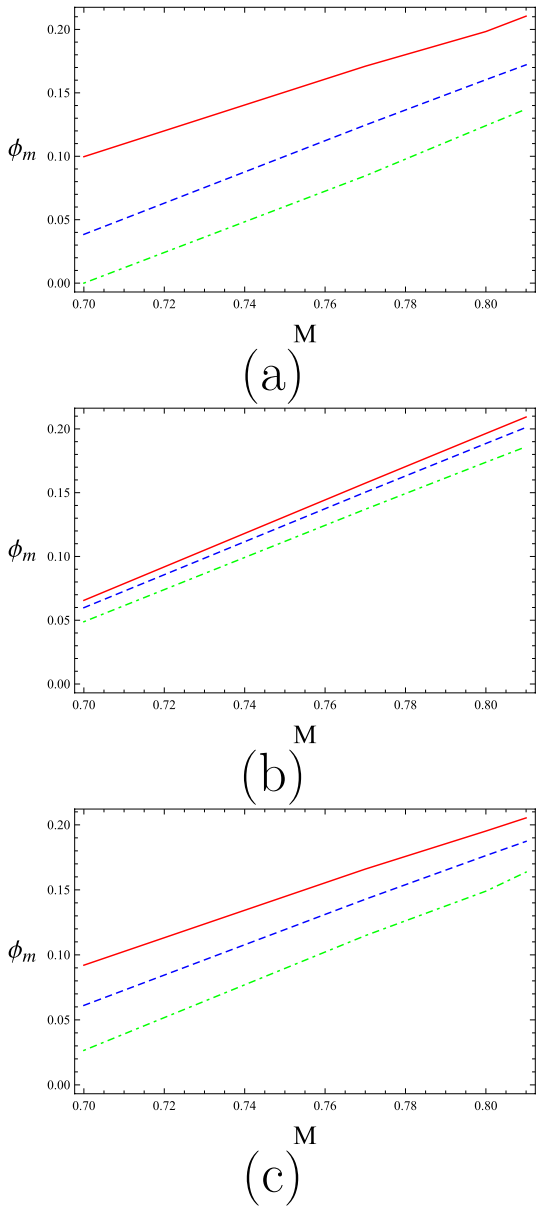

Fig. 7. Soliton amplitude ϕ_m (determined as the root of $V(\phi_m)$) is plotted against various parameters, satisfying the results shown in Figs. 3–6. (a) Variation of ϕ_m versus the Mach number M for different values of p. Dotted-dashed curve: $p = 0.05$; dashed curve: $p = 0.1$; and solid curve: $p = 0.2$, where other parameters are $\eta_{e0} = 2$ and $g_i = 0.03$. (a) Variation of ϕ_m versus the Mach number M for different values of g_i. Solid curve: $g_i = 0.005$; dashed curve: $g_i = 0.01$; and dotted-dashed curve: $g_i = 0.02$, where $\eta_{e0} = 2$ and $p = 0.1$. (c) Variation of ϕ_m versus M for different values of η_{e0}. Solid curve: $\eta_{e0} = 1.75$; dashed curve: $\eta_{e0} = 1.90$; and dotted-dashed curve: $\eta_{e0} = 2.05$. Here, $g_i = 0.03$ and $p = 0.1$.

The numerical outcome for the electrostatic potential forms (pulses), to be numerically obtained by solving the pseudobalance equation, as explained above, for the relevant parameter values, are here omitted for brevity.

VI. Conclusion

To conclude, we have investigated the linear and nonlinear ion-acoustic waves in an unmagnetized collisionless degenerate e–p–i plasma, composed of relativistically degenerate electrons and positrons, whereas the ions are warm and nondegenerate, whose inertia is retained.

At a first step, a linear analysis has shown that the dispersion properties of ion-acoustic waves are strongly influenced by the relevant parameters, namely, the positron content (p), the ionic thermal effect (via g_i), and the electron relativity parameter (via η_{e0}).

Adopting the reductive perturbation method, we have derived a KdV-type partial differential equation, and then solved it to obtain an exact analytical expression for small amplitude weakly super-acoustic solitary waves. We have pursued our analysis by extending it to account for large (arbitrary) amplitude ion-acoustic solitary waves, and have derived an pseudomechanical energy-balance equation governing the dynamics of localized pulses.

Only positive electrostatic potential excitations (solitary waves) were found to exist. The existence domain, wherein the solitary waves may occur, was determined and analyzed numerically. It was found that the existence region shrinks with increasing positron concentration (value of p) and, independently, ion temperature (via g_i). On the other hand, higher values of η_{e0} lead to a broader allowable soliton existence domain, hence allowing for faster ion acoustic solitary waves. It is interesting to mention that extremely high values of η_{e0} (in the strongly relativistic case) allows only supersonic solitary waves.

We have relied in our investigation on a model which has been adopted in a variety of earlier works, combining the relativistic Chandrasekhar [6] pressure term into a classical fluid description. We may add, for rigor, that this model is valid for moderately relativistic regimes (as it basically relies on a classical 1-D fluid model), yet is here adopted for its simplicity. A more elaborate fully relativistic model for electrostatic waves is being developed, and will be reported soon [23].

This paper is of relevance to white dwarf stars [1], where a series of established theories have predicted the existence of acoustic-type modes [24], [25], in which ions provide the inertia and mainly the electron degeneracy pressure provides the restoring force. Although the existence of such modes was predicted very early [26], these have not been observed so far [25]. The lack of observations does not imply the absence of acoustic modes, but may be associated with plasma motion below the detection limit [24]. The possibility of the formation of finite amplitude acoustic waves is also suggested in the case of extreme events, such as supernova explosions [4], [24]. Abundant theoretical investigations of relevance to this context have been proposed [8]–[15], [20].

It appears imposed and timely to add that a number of sophisticated experiments have recently been carried out to demonstrate the possibility for positron production during the interaction of ultrahigh intensity ultrashort laser pulses with solid targets (laser–matter interaction), which gives rise to high-density plasma entering the quantum regime [19], [27]–[29]. Although admittedly at a somewhat speculative stage, we anticipate that our results will be relevant with electrostatic oscillations observed during those experiments.

Our investigation can be generalized by including the ambient magnetic field, in which we have the possibility to study the magnetosonic solitons [30] in degenerate plasmas.

APPENDIX A
DERIVATION OF (7)

We consider the electron momentum equation (3)

$$en_e\frac{\partial\phi}{\partial x}-\frac{\partial P_e}{\partial x}=0. \tag{A1}$$

We have

$$\begin{aligned}\frac{1}{n_e}\frac{\partial P_e}{\partial x}&=\frac{1}{n_e}\frac{dP_e}{dn_e}\frac{dn_e}{d\eta_e}\frac{\partial\eta_e}{\partial x}\\&=\frac{m_ec^2\eta_e}{\left(1+\eta_e^2\right)^{\frac{1}{2}}}\frac{\partial\eta_e}{\partial x}\\&=\frac{\partial}{\partial x}\left(m_ec^2\sqrt{1+\eta_e^2}\right).\end{aligned} \tag{A2}$$

Integrating (A1), we obtain

$$\begin{aligned}\int_{-\infty}^{x}\frac{\partial\phi}{\partial z}dz&=\frac{1}{en_e}\int_{-\infty}^{x}\frac{\partial P_e}{\partial z}dz\\\phi&=\frac{m_ec^2}{e}\left[\left(1+\eta_e^2\right)^{\frac{1}{2}}-\left(1+\eta_{e0}^2\right)^{\frac{1}{2}}\right].\end{aligned}$$

Rearranging, and solving for η_e

$$\eta_e=\pm\left\{\left[\frac{e\phi}{m_ec^2}+\left(1+\eta_{e0}^2\right)^{\frac{1}{2}}\right]^2-1\right\}^{\frac{1}{2}} \tag{A3}$$

and then, recalling the definition of η_e, hence solving for n_e (adopting the positive sign to preserve the positive of $n_e>0$), (A3) gives

$$n_e=\frac{8\pi m_e^3c^3}{3h^3}\left[\frac{e^2\phi^2}{m_e^2c^4}+\frac{2e\phi}{m_ec^2}\left(1+\eta_{e0}^2\right)^{\frac{1}{2}}+\eta_{e0}^2\right]^{\frac{3}{2}}. \tag{A4}$$

The same method is employed to express the positron number density in terms of the electrostatic potential ϕ, upon a trivial sign change: the first term in (A1) is preceded by a minus sign, due to the positron (positive) charge. Algebraically speaking, this is formally tantamount to setting $\phi\rightarrow-\phi$ everywhere in this appendix. Therefore, the final expression for positrons reads

$$n_p=\frac{8\pi m_p^3c^3}{3h^3}\left[\frac{e^2\phi^2}{m_p^2c^4}-\frac{2e\phi}{m_ec^2}\left(1+\eta_{p0}^2\right)^{\frac{1}{2}}+\eta_{p0}^2\right]^{\frac{3}{2}}. \tag{A5}$$

Equations (A4) and (A5) combined lead to (7) in the text.

APPENDIX B
PAIR ANNIHILATION

Electrons and positrons tend to annihilate mutually, via various annihilation mechanisms. Pair annihilation results in gamma-ray photon production [1]

$$e^+ + e^-\rightarrow\gamma+\gamma'. \tag{B1}$$

To study the collective behavior of a plasma containing electrons and positrons via a fluid description, it is necessary to satisfy certain criteria for annihilation processes to be neglected. As a matter of fact, e–p pair annihilation becomes unimportant when the following inequality is satisfied:

$$\omega_{p,j}^{-1}\ll\tau_{\text{ann}} \tag{B2}$$

where $\omega_{p,j}^{-1}$ is the inverse of the plasma frequency and τ_{ann} is the annihilation time. The annihilation time τ_{ann} in the relativistic regime can be expressed by the following relation [1]–[3]:

$$\tau_{\text{ann}}=\frac{4}{3}\frac{1}{n_j\,\sigma_\tau\,c}\left(\frac{\Theta^2}{\frac{1}{4}+\ln(2\delta\Theta+1)}\right)\quad\text{for }\Theta\gg1 \tag{B3}$$

where $\sigma_\tau(=6.65\times10^{-25}\ \text{cm}^2)$ is the electron Thompson cross section and $\Theta(=k_BT_{Fj}/m_jc^2)$ is the normalized thermal energy. Furthermore, $\delta=e^{-\Xi_E}\equiv0.5615$ with $\Xi_E(\approx0.5772)$ the Euler's constant. Combining (B2) and (B3), while using $n_{e0}\simeq n_{p0}=n_0$, the pair annihilation condition becomes

$$\left(\frac{\Theta^2}{\frac{1}{4}+\ln(1.123\,\Theta+1)}\right)\gg2.6\times10^{-19}\,n_0^{\frac{1}{2}}. \tag{B4}$$

It is important to mention that (B4) is well satisfied for the typical mass density range $\rho\sim10^6$ g/cm^{-3}, which is characteristic of relativistic dense plasmas found in astrophysical environments (viz., white dwarfs). This clearly shows that e–p pair annihilation can be ignored and thus the study of ion acoustic waves can be carried out safely in a dense plasma configuration, as studied in this paper.

ACKNOWLEDGMENT

A. ur Rahman would like to thank M. Mc Kerr, Queen's University Belfast, Belfast, U.K., for his support and assistance.

REFERENCES

[1] D. Koester and G. Chanmugam, "Physics of white dwarf stars," *Rep. Prog. Phys.*, vol. 53, no. 7, pp. 837–915, 1990.

[2] S. L. Shapiro and S. A. Teukolsky, *Black Holes, White Dwarfs and Neutron Stars: The Physics of Compact Objects*. New York, NY, USA: Wiley, 1983.

[3] G. Chabrier, F. Douchin, and A. Y. Potekhin, "Dense astrophysical plasmas," *J. Phys., Condens. Matter*, vol. 14, no. 40, pp. 9133–9139, 2002.

[4] V. E. Fortov, "Extreme states of matter on earth and in space," *Phys.-Uspekhi*, vol. 52, no. 6, pp. 615–647, 2009.

[5] P. K. Shukla and B. Eliasson, "*Colloquium*: Nonlinear collective interactions in quantum plasmas with degenerate electron fluids," *Rev. Modern Phys.*, vol. 83, no. 3, pp. 885–906, Sep. 2011.

[6] S. Chandrasekhar, *Philosophical Magazine*, vol. 11. 1931, p. 592.

[7] S. Chandrasekhar, *An Introduction to the Study of Stellar Structure*. Chicago, IL, USA: Univ. Chicago Press, 1939.

[8] A. A. Mamun and P. K. Shukla, "Solitary waves in an ultrarelativistic degenerate dense plasma," *Phys. Plasmas*, vol. 17, no. 10, p. 104504, 2010.

[9] W. Masood and B. Eliasson, "Electrostatic solitary waves in a quantum plasma with relativistically degenerate electrons," *Phys. Plasmas*, vol. 18, no. 3, p. 034503, 2011.

[10] A.-U. Rahman, S. Ali, A. Mushtaq, and A. Qamar, "Nonlinear ion acoustic excitations in relativistic degenerate, astrophysical electron–positron–ion plasmas," *J. Plasma Phys.*, vol. 79, no. 5, pp. 817–823, 2013.

[11] A.-U. Rahman, S. Ali, A. M. Mirza, and A. Qamar, "Planar and non-planar ion acoustic shock waves in relativistic degenerate astrophysical electron-positron-ion plasmas," *Phys. Plasmas*, vol. 20, no. 4, p. 042305, 2013.

[12] M. Akbari-Moghanjoughi, "Propagation of arbitrary-amplitude ion waves in relativistically degenerate electron-ion plasmas," *Astrophys. Space Sci.*, vol. 332, no. 1, pp. 187–192, 2011.
[13] R. Sabry, W. M. Moslem, and P. K. Shukla, "Freak waves in white dwarfs and magnetars," *Phys. Plasmas*, vol. 19, no. 12, p. 122903, 2012.
[14] I. Kourakis, M. McKerr, and A.-U. Rahman, "Semiclassical relativistic fluid theory for electrostatic envelope modes in dense electron–positron–ion plasmas: Modulational instability and rogue waves," *J. Plasma Phys.*, vol. 79, no. 6, pp. 1089–1094, 2013.
[15] M. McKerr, I. Kourakis, and F. Haas, "Freak waves and electrostatic wavepacket modulation in a quantum electron–positron–ion plasma," *Plasma Phys. Controlled Fusion*, vol. 56, no. 3, p. 035007, 2014.
[16] H. Washimi and T. Tanuiti, "Propagation of ion-acoustic solitary waves of small amplitude," *Phys. Rev. Lett.*, vol. 17, pp. 996–998, Nov. 1966.
[17] R. Z. Sagdeev, "Cooperative phenomena and shock waves in collisionless plasmas," in *Reviews of Plasma Physics*, vol. 4, M. A. Leontovich, Ed. New York, NY, USA: Consultants Bureau, 1966, p. 23.
[18] H. Chen *et al.*, "Relativistic positron creation using ultraintense short pulse lasers," *Phys. Plasmas*, vol. 16, p. 122702, Mar. 2009.
[19] G. Sarri *et al.*, "Table-top laser-based source of femtosecond, collimated, ultrarelativistic positron beams," *Phys. Rev. Lett.*, vol. 110, p. 255002, Jun. 2013.
[20] W. F. El-Taibany and A. A. Mamun, "Nonlinear electromagnetic perturbations in a degenerate ultrarelativistic electron-positron plasma," *Phys. Rev. E*, vol. 85, p. 026406, Feb. 2012.
[21] T. Dauxois and M. Peyrard, *Physics of Solitons*. Cambridge, U.K.: Cambridge Univ. Press, 2006.
[22] S. S. Ghosh, K. K. Ghosh, and A. N. S. Iyengar, "Large mach number ion acoustic rarefactive solitary waves for a two electron temperature warm ion plasma," *Phys. Plasmas*, vol. 3, no. 11, pp. 3939–3946, 1996.
[23] F. Haas and I. Kourakis, "Relativistic hydrodynamic equations for fully degenerate plasma," in *Proc. Int. Congr. Plasma Phys. (ICPP)*, Lisbon, Portugal, Sep. 2014, pp. 1–9.
[24] B. Eliasson and P. K. Shukla, "The formation of electrostatic shocks in quantum plasmas with relativistically degenerate electrons," *Europhys. Lett.*, vol. 97, no. 1, pp. 15001–15005, 2012.
[25] R. Silvotti *et al.*, "Search for p-mode oscillations in DA white dwarfs with VLT-ULTRACAM," *Astron. Astrophys.*, vol. 525, Jan. 2011, Art. ID A64.
[26] J. P. Ostriker, "Recent developments in the theory of degenerate dwarfs," *Annu. Rev. Astron. Astrophys.*, vol. 9, pp. 353–366, Sep. 1971.
[27] G. Sarri *et al.*, "Laser-driven generation of collimated ultra-relativistic positron beams," *Plasma Phys. Controlled Fusion*, vol. 55, no. 12, p. 124017, 2013.
[28] G. Sarri *et al.*, "Generation of neutral and high-density electron-positron pair plasmas in the laboratory," *Nature Commun.*, to be published.
[29] G. Sarri *et al.*, "Laser-driven generation of electron-positron beams: A review," *J. Plasma Phys.*, to be published.
[30] M. Marklund, B. Eliasson, and P. K. Shukla, "Magnetosonic solitons in a fermionic quantum plasma," *Phys. Rev. E*, vol. 76, pp. 067401–067404, Dec. 2007.
[31] R. Svensson, "Electron-positron pair equilibria in relativistic plasmas," *Astrophys. J.* vol. 258, pp. 335–348, Jul. 1982.

Ata ur Rahman was born in Nowshera, Pakistan, in 1985. He received the M.Sc. degree in physics and the Ph.D. degree in plasma physics from the Department of Physics, University of Peshawar, Peshawar, Pakistan, in 2007 and 2014, respectively.

He is currently an Assistant Professor of Physics with the Department of Physics, Islamia College Peshawar, Peshawar. His current research interests include nonlinear dynamics, solitary waves/shocks with emphasis on applications to dense astrophysical regimes, and superintense laser-dense matter experiments.

Mr. Rahman is a Lifetime Member of the Pakistan Physical Society.

Ioannis Kourakis was born in Crete, Greece. He received the B.Sc. degree in physics from the University of Crete, Heraklion, Greece, the D.E.A. (French M.Sc. equivalent) degree in molecular spectroscopy and material science from the University of Burgundy, Dijon, France, the the D.E.A. (Belgian M.Phil. equivalent) degree in science, and the Ph.D. degree in Theoretical Physics, both from the Free University of Brussels, Brussels, Belgium.

He currently holds an academic position with the Centre for Plasma Physics, Queen's University Belfast, Belfast, U.K. He has earlier carried out research and teaching work with the University of Burgundy, the Free University of Brussels, Gent University, Ghent, Belgium, and Ruhr University, Bochum, Germany. He has authored approximately 200 papers in refereed journals and conference proceedings, which have attracted more than 2000 citations. His current research interests include nonlinear physics, with emphasis on laser-plasma interactions, dusty (complex) plasmas, space plasmas, quantum plasmas, and materials science.

Dr. Kourakis is a member of the American Physical Society, the U.K. Institute of Physics, the American Geophysical Union, and the Hellenic Astronomical Society (Greece).

Anisa Qamar was born in Mardan, Pakistan, in 1968. She received the M.Sc. degree in physics from the Department of Physics, University of Peshawar, Peshawar, Pakistan, in 1992, and the Ph.D. degree in plasma physics from Quaid-i-Azam University, Islamabad, Pakistan, in 2004.

She is currently an Associate Professor of Physics with the Department of Physics, University of Peshawar. She has made significant contributions to the field of dusty plasmas She has authored over 30 research articles in international journals. Her current research interests include the nonlinear dynamics and coherent nonlinear structures (solitons, shocks, double layers, etc.) in classical as well as in degenerate dense plasmas.